

Timescales of decay by tunneling of a localized state

Y. Ban¹, E. Ya. Sherman^{1,2}, J. G. Muga¹, and M. Büttiker³

¹*Department of Physical Chemistry, Universidad del País Vasco UPV-EHU, 48080 Bilbao, Spain*

²*Basque Foundation for Science IKERBASQUE, 48011, Bilbao, Spain*

³*Département de Physique Théorique, Université de Genève, CH-1211 Genève 4, Switzerland*

Motivated by recent time domain experiments on atom ionization, we analyze the transients and timescales that characterize, besides the relatively long lifetime, the decay by tunneling of a localized state through a moderately opaque rectangular barrier. In particular the time dependence of the flux and density at the edges of a barrier at short times, when the tunneling process is forming, is investigated. This short-term behavior depends strongly on the initial state. The tunneling starts immediately, however, some time is required for the outgoing flux to develop. Then a quasistationary, slowly decaying process follows, which sets ideal conditions for observing diffraction in time at longer times and distances. We also extrapolate backwards the propagation of the wave packet escaped from the potential to define operationally a tunnelling time at the barrier edge. This extrapolated time is considerably longer than the timescale of the flux or density buildup at the barrier edge. When the initial state is tightly localized so that the initial transients are dominated by over-the-barrier motion, the timescale for the flux propagation through the barrier is close to the Büttiker-Landauer traversal time.

PACS numbers: 03.65.Nk, 03.65.Xp, 03.75.-b

I. INTRODUCTION

Tunneling is one of the most fundamental concepts in quantum mechanics. At a microscopic single-particle scale it deals with phenomena such as α -decay in nuclear physics [1] and ionization of atoms [2] by pulses of strong electric fields in quantum optics. The field of applications where the tunneling plays the crucial role includes quantum solid-state transport devices [3, 4] and cascade lasers [5]. The recent discovery of atomic Bose-Einstein condensates renewed interest in macroscopic tunneling effects [6].

Since MacColl [7] pointed out in 1932 that tunneling is not only characterized by an integral probability but also by the time that the particle takes to traverse the barrier, several relevant time scales have been put forward. Despite a rich research history, the question of how long it takes for a particle to tunnel through a barrier is still debated and investigated experimentally. A typical setting is the scattering process, where a wavepacket is reflected from and transmitted through a barrier higher than the incident particle energy. In this case, the group delay [8], defined in terms of the energy derivatives of the reflection or transmission phase shift, describes the motion of the wave packet peak. It was also found that the group delay for particles tunneling through an opaque barrier is independent of the barrier width (the ‘‘Hartman effect’’ [9]), which can be related to the saturation of the integrated probability density (or number of particles) under the barrier [10]. With the development of electron devices, the group delay has been a quantity of interest in quantum coherent electron transport as it is closely related to the density of states [11] as well as to the maximum operational rate of such devices [12, 13]. Interestingly, in graphene, a single layer of Carbon atoms, where transport is via evanescent waves, the Wigner-Smith delay is nevertheless *linear* in the tunneling distance [14, 15]. The dwell time [16, 17], was introduced as a measure of the average time spent by a particle in a given region. An approach proposed by Baz and Rybachenko [18, 19] uses the Larmor precession as a clock to measure the time spent by a particle with a magnetic moment in a weak magnetic field. In classically forbidden regions there is not only precession but also a rotation [17] of the moment into the direction of the field. In 1982, Büttiker and Landauer [20] reviewed the tunneling time scales in the scattering problem. Analyzing tunneling through an oscillating barrier they found an interaction time which is closely related to the rotation of the magnetic moment [17, 20]. Recent interest in systems with strong spin-orbit coupling leads to related questions [21, 22] .

Tunneling times in one and two dimensions have been investigated [23] by using the analogy between the time-

independent Schrödinger equation and the Helmholtz equation in electrodynamics. Brouard, Sala, and Muga, using scattering theory projectors for to-be-transmitted/reflected wavepacket parts and for localizing the particle at the barrier, set a formal framework that unified many of the existing proposals pointing out that the multiple time scales correspond to different quantizations of the classical transmission time, due to the noncommuting observables and possible orderings involved [24]. This clarified the meaning of different partitions of the dwell time into transmitted, reflected and interference components. Another research line has been the investigation of characteristic times for the transient dynamics of the wave function (e.g. the forerunners) in a plethora of potential configurations and initial conditions using asymptotic methods [24–26]. For specially prepared states, in particular for confined or semiconfined initial waves with a flat density, these transients show diffraction in time (DIT) [26, 27], i.e. temporal oscillations reminiscent of spatial Fresnel-diffraction by a sharp edge [27].

Early experiments have extracted a time scale for tunneling in Josephson junctions coupled to transmission lines of variable length [28] and for electron tunneling through extremely low barriers in semiconductor heterostructures [29]. Tunneling times can be inferred from the width of field-emission microscopy images of ions using the perpendicular momentum distribution as a clock [30]. A tunneling time has been measured for electromagnetic waves, including passing through optical barriers [31], photonic band gap structures [32] consisting of alternating layers with different refraction indices, and microwaves tunneling through waveguides [33, 34].

An important tunneling-dependent phenomenon is the decay of a metastable system [35–38]. Compared to the full scattering problem, the decay configuration, or “half-scattering” problem, has been frequently considered unproblematic because of the absence of the transmitted/reflected wavepacket splitting and the existence of a well known temporal characterization in terms of resonance lifetimes. In fact, one may still pose classically minded questions on the tunnelling time similar to the ones in the scattering configuration, however, without obvious answers. A particle may wander in the trapping well for a while and then escape through the barrier. For such a “history” the lifetime would be the addition of the waiting time in the well plus the tunneling time. Can this quantity be defined and measured in a sensible way? The understanding can be based on the analysis of quantum interference among the Feynman paths [39] or on the consideration of the quantities defined by operational procedures, as presented in this paper.

In recent years, the techniques of atom ionization by a strong laser field and attosecond probing of electron dynamics

opened a new venue for experimental studies of the tunneling times. The measurement of ionization of He atoms [2] has allowed to observe the tunneling delay of electrons in real time. In this experiment the tunneling delay time was defined as the interval between the lowering of the Coulomb barrier and the instant at which the escaping electron first experiences acceleration by the laser field. On the mesoscopic scale, a process analogous to ionization consists in the charging and discharging of a capacitor, a small cavity coupled with a single tunnel barrier to a metallic contact [40]. An oscillating potential applied to the cavity leads to the emission of electrons and holes with small probability in the linear response regime [41, 42] and with probability one under large amplitude voltage pulses [43–45]. A broader discussion of the dynamics of such a capacitor is given in Ref. [46].

The aim of this paper is to further explore and clarify the dynamics of the tunneling-induced decay of localized states. A simple quantum mechanical model, which simulates the experimental measurement of tunneling time, allowing for opening and closing the barrier [2], is introduced. Different from the scattering problem, the initial state we prepare propagates and decays through the barrier. We calculate the probability density and flux to study the short-term dynamics near the barrier and the long-term dynamics far away from it. For an opaque barrier we observe a relatively short transient time scale, where the tunneling is developed into a quasi steady (decaying) process. The details of the initial state have an important impact on the transients.

At large distances, the flux and the density start to grow at long times, reach a peak and then decrease by diffraction-in-time oscillations. This provides a useful route for their elusive observation. As these two quantities are measurable, it is possible to suggest an operational definition of the tunneling time, similar to the definition in the experiment [2]. The tunneling time obtained using this approach by extrapolating the particle motion from the position of the remote detector to the right edge of the barrier is not directly related to the timescale of the flux or density buildup there. We also study the influence of the closing time when the tunneling process is terminated on that operationally defined tunneling time.

II. MODEL

We consider the following model of the potential $U(x, t)$. At $t < 0$, the potential $U_1(x)$ is a step in the positive half-axis, with zero potential energy at $0 < x < a_1$ and U_0 at $x > a_1$, while there is an infinitely high wall at $x < 0$,

as shown in Fig.1(a). We assume that this potential can hold bound states. At $t = 0$ the potential changes to $U_2(x)$, which is a barrier extended from a_1 to a_2 with the same height U_0 , as shown in Fig. 1(b). At $t = t_0$ the potential changes back to its initial form so that the entire time dependence is

$$U(x, t) = \begin{cases} U_1(x) & (t < 0 \text{ and } t > t_0), \\ U_2(x) & (0 < t < t_0). \end{cases} \quad (1)$$

The initial state $\Psi(x, t = 0)$ prepared at $t = 0$ starts to decay at $t > 0$. This is similar to the ionization of an atom by the application of a strong laser field, which lets a valence electron to tunnel through the barrier. At the closing time t_0 , the potential becomes $U_1(x)$ again and the decay terminates. For simplicity, we apply dimensionless variables, using the length unit $a_1 \equiv 1$ and setting $\hbar \equiv m \equiv 1$. As a result, the time, momentum, and energy are measured in the corresponding units.

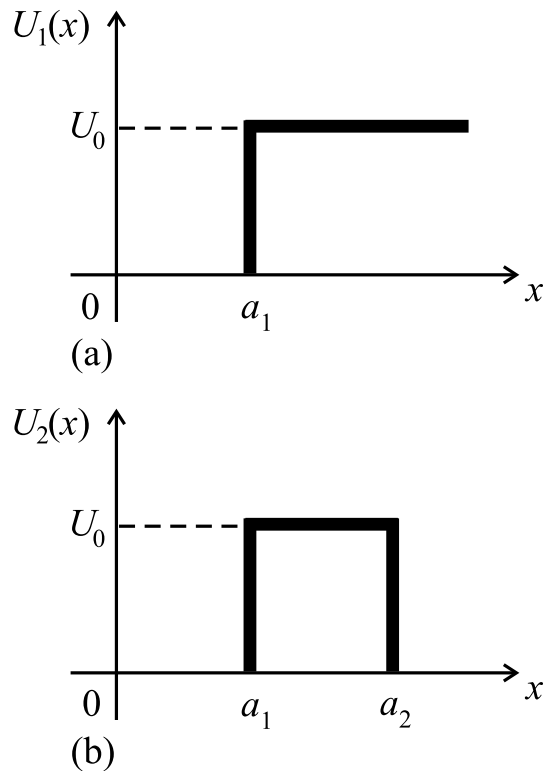


FIG. 1. The time-dependent potential function is $U_1(x)$ at $t = 0$ and $t > t_0$, $U_2(x)$ within the interval $0 < t < t_0$. (a) shows that $U_1(x)$ is a step in the positive-half plane, which is 0 from $x = 0$ to $x = a_1$ and U_0 from $x = a_1$ to infinity, while (b) presents a barrier which extends from $x = a_1$ to $x = a_2$ and is of height of U_0 . The potential energy is always infinite in the negative halfplane.

The eigenstate of the Hamiltonian corresponding to $U_2(x)$ is

$$\phi_k(x) = \begin{cases} C(k) \sin(kx), & (0 < x < a_1) \\ D(k) \exp(-\kappa_k x) + F(k) \exp(\kappa_k x), & (a_1 < x < a_2) \\ \sqrt{2/\pi} \sin[kx + \theta(k)], & (x > a_2) \end{cases} \quad (2)$$

with the normalization condition $\langle \phi_{k'} | \phi_k \rangle = \delta(k - k')$. The coefficients $C(k)$, $D(k)$, $F(k)$ and the phase $\theta(k)$ satisfy the boundary conditions of the potential $U_2(x)$, and $\kappa_k = \sqrt{2U_0 - k^2}$. In the tunneling regime $k < \sqrt{2U_0}$, while in the propagating regime $k > \sqrt{2U_0}$, $i\kappa_k$ is substituted by k' , where $k' = \sqrt{k^2 - 2U_0}$.

In the time interval $0 < t < t_0$ the wave function $\Psi(x, t)$ can be expressed as

$$\Psi(x, 0 < t < t_0) = \int_0^\infty G(k) \phi_k(x) \exp\left(-\frac{ik^2 t}{2}\right) dk, \quad (3)$$

where k is the wavenumber, with

$$G(k) = \int_0^\infty \Psi(x, 0) \phi_k^*(x) dx, \quad (4)$$

where superscript $*$ represents the complex conjugate.

Let us set the initial state as the ground state of the Hamiltonian corresponding to $U_1(x)$. For example, for $U_0 = 16$ there are two bound eigenstates: the ground state $\varphi_0(x)$ (energy E_0) and the first excited state $\varphi_1(x)$ (energy E_1). The continuum states with $U_1(x)$ are denoted as $\varphi_k(x)$ to be distinguished from the states ϕ_k corresponding to $U_2(x)$. The energy E_0 (at $t = -\epsilon$, where $\epsilon \rightarrow 0$) for $\Psi(x, 0) = \varphi_0(x)$ is 3.52. Since $\kappa d = 2$ (with $\kappa \equiv \sqrt{2(U_0 - E_0)}$ and $d \equiv a_2 - a_1$) this barrier can be considered as a moderately opaque one. To clarify the influence of initial states on the tunneling, we alter the initial state into the ground state of an infinite-wall potential, $\Psi(x, 0) = \sqrt{2} \sin(\pi x)$. Therefore, E_0 is $\pi^2/2$ and a_2 becomes 1.42 to keep κd unchanged. As shown in Fig. 2, the coefficient $G(k)$ has contributions of two resonances corresponding to the bound states of the initial potential. For $\Psi(x, 0) = \varphi_0(x)$, the second one is extremely weak.

After closing the barrier at $t = t_0$, the potential becomes the original step again, and the wave function can be expressed as

$$\Psi(x, t > t_0) = B_0 \varphi_0(x) \exp[-iE_0(t - t_0)] + B_1 \varphi_1(x) \exp[-iE_1(t - t_0)] + \int_{\sqrt{2U_0}}^\infty B(k) \varphi_k(x) \exp\left[-\frac{ik^2(t - t_0)}{2}\right] dk \quad (5)$$

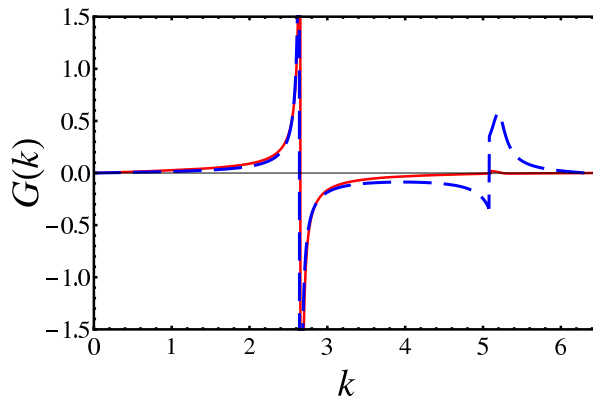


FIG. 2. The coefficient $G(k)$, where the solid line and the dashed line correspond to the initial states $\Psi(x, 0) = \varphi_0(x)$ with $a_2 = 1.4$ and $\Psi(x, 0) = \sqrt{2}\sin(\pi x)$ with $a_2 = 1.42$, respectively. In both cases, $\kappa d = 2$ and $U_0 = 16$.

with

$$B_{0,1} = \int_0^\infty \Psi(x, t_0) \varphi_{0,1}^*(x) dx, \quad (6)$$

$$B(k) = \int_0^\infty \Psi(x, t_0) \varphi_k^*(x) dx. \quad (7)$$

For $k > \sqrt{2U_0}$ the eigenstates have the form:

$$\varphi_k(x) = \begin{cases} C_1(k) \sin(kx), & (0 < x < a_1) \\ \sqrt{2/\pi} \sin[qx + \theta_1(k)], & (x > a_1) \end{cases} \quad (8)$$

where $q = \sqrt{k^2 - 2U_0}$ with $C_1(k)$ and $\theta_1(k)$ determined by the boundary conditions at $x = a_1$. With Eqs. (3) and (5) we have specified the time-evolution of our dynamic escape problem.

III. RESULTS

A. Decay and Survival

The decay rate is described by the probability to find the particle in the well from $x = 0$ to $x = a_1$ defined as

$$w_1(t) = \int_0^{a_1} \Psi^*(x, t) \Psi(x, t) dx. \quad (9)$$

The life time $t_{1/e}$, an important time scale introduced to characterize the decay rate, is the time that it takes for the relative probability in the well $w_1(t)/w_1(0)$ to decay to $1/e$. Quite generally the decay time can be written

approximately as $t_{1/e} \approx AT_{k_0} \exp(2\kappa d)$, where $k_0 = \sqrt{2E_0}$, $T_{k_0} = 2/k_0$ is the period of motion for a particle in the well, $\exp(-2\kappa d)$ is the tunneling rate, and A is a barrier-dependent coefficient of order 1. Therefore, κd is a significant physical parameter with regard to the decay process and the tunneling time. Under the conditions of $\Psi(x, 0) = \varphi_0(x)$, $U_0 = 16$, $a_2 = 1.4$, the life time is $t_{1/e} = 17.5$.

Another quantity is the survival probability

$$S(t) = \left| \int_0^\infty \Psi^*(x, 0) \Psi(x, t) dx \right|^2 \quad (10)$$

to remain in the initial state [36]. The decay of $w_1(t)$ and $S(t)$ are shown in Fig. 3 for different model parameters keeping κd constant.

Although all the probabilities decrease exponentially at long times, the ones with $\Psi(x, 0) = \sqrt{2} \sin(\pi x)$ in Fig. 3(b) and (d) oscillate fast, while those with $\Psi(x, 0) = \varphi_0(x)$ in (a) and (c) decay smoothly. This is because $\Psi(x, 0) = \sqrt{2} \sin(\pi x)$ has a significant contribution of the second resonance shown in Fig. 2 leading to interference with the “ground state” resonance. Another difference is that $w_1(0) = 1$ for $\Psi(x, 0) = \sqrt{2} \sin(\pi x)$, while $w_1(0) < 1$ for $\Psi(x, 0) = \varphi_0(x)$, as the latter one is not fully localized in the well initially.

B. Short-term dynamics

In this subsection we address the problem of “how the tunneling begins ?” by studying the short-time dynamics of the flux

$$J(x, t) = \frac{1}{2i} \left[\Psi^*(x, t) \frac{\partial \Psi(x, t)}{\partial x} - \frac{\partial \Psi^*(x, t)}{\partial x} \Psi(x, t) \right], \quad (11)$$

and the density,

$$\rho(x, t) = \Psi^*(x, t) \Psi(x, t). \quad (12)$$

These two quantities satisfy the continuity equation

$$\frac{\partial \rho(x, t)}{\partial t} + \frac{\partial J(x, t)}{\partial x} = 0. \quad (13)$$

Based on Eq. 13, we obtain the flux at the edges,

$$J(a_1, t) = -\frac{dw_1(t)}{dt}, \quad J(a_2, t) = \frac{dw_2(t)}{dt}, \quad (14)$$

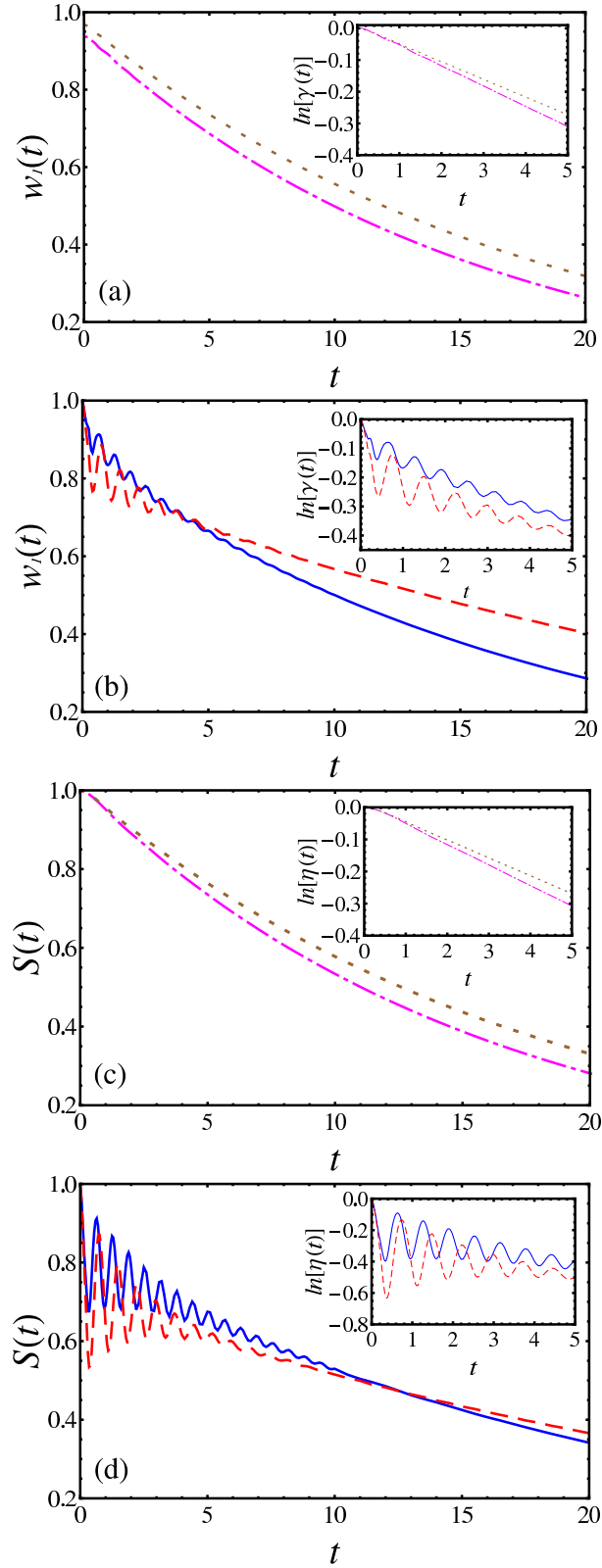


FIG. 3. The probability [(a),(b)] to find the particle in the well from 0 to a_1 and the survival probability [(c), (d)] to remain in the initial state. The dotted and the dot-dashed lines are for two initial states $\Psi(x,0) = \varphi_0(x)$, one for $U_0 = 16$ $a_2 = 1.4$ and the other for $U_0 = 10$, $a_2 = 1.54$. The solid and the dashed lines represent the barriers $U_0 = 16$, $a_2 = 1.42$ and $U_0 = 10$, $a_2 = 1.63$ with the same initial state $\Psi(x,0) = \sqrt{2} \sin(\pi x)$. The insets exhibit $\ln[\gamma(t)]$ and $\ln[\eta(t)]$ at small time scale, where $\gamma(t) \equiv w_1(t)/w_1(0)$ and $\eta(t) \equiv S(t)/S(0)$.

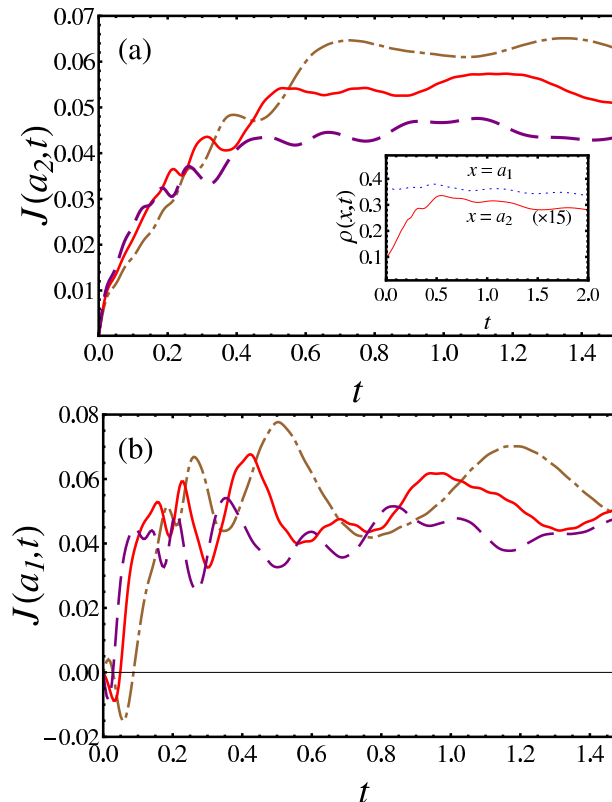


FIG. 4. (a) Flux at the right edge a_2 . The dashed, solid and dot-dashed lines correspond to the barriers $U_0 = 24$ ($a_2 = 1.31$), $U_0 = 16$ ($a_2 = 1.4$), $U_0 = 10$ ($a_2 = 1.54$), respectively. The inset presents the density at a_1 (dotted) and multiplied by fifteen at a_2 (solid), with the barrier $U_0 = 16$, $a_2 = 1.4$. (b) Flux at the left edge a_1 . All lines correspond to the same parameters as those in (a). For all plots $\kappa d = 2$, and $\Psi(x, 0) = \varphi_0(x)$.

where

$$w_2(t) = \int_{a_2}^{\infty} \Psi^*(x, t) \Psi(x, t) dx \quad (15)$$

is the probability to find the particle outside the potential.

In Fig. 4, we illustrate the time dependence of the edge flux for different barriers during a short time scale for $\Psi(x, 0) = \varphi_0(x)$. It can be seen from Fig. 4(a) that $J(a_2, t)$ increases during a short time interval and then reaches a rough plateau. The lines shift to the right by lowering the barrier. The time scale when $J(a_2, t)$ becomes the plateau also becomes larger, although it cannot be defined precisely. A crude estimate for this scale is $\pi/(2E_0)$, in a good agreement with the results presented in Fig.4(a). Even though the numerically estimated times are much shorter, a similar trend in variation with the height of the barrier is shown by the Büttiker-Landauer time (BL time), provided

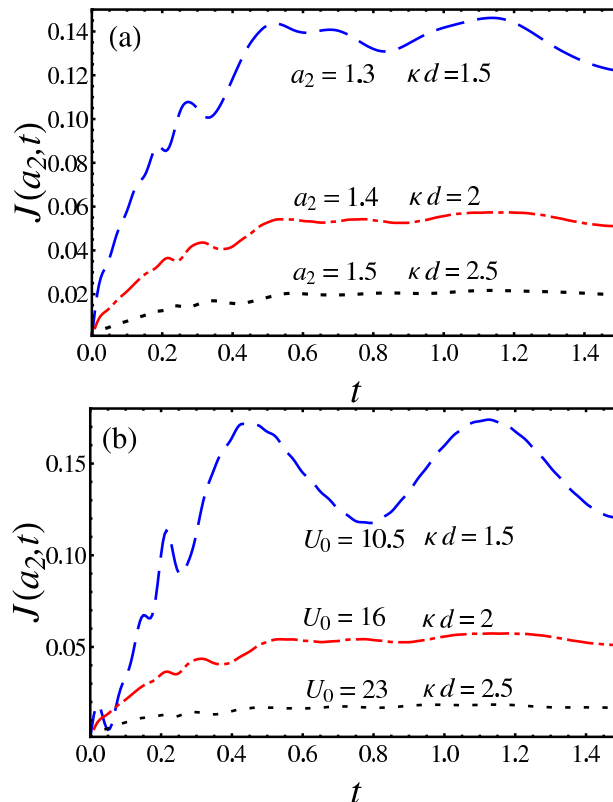


FIG. 5. (a) Flux at the right edge on time with different width $a_2 = 1.3$ (dashed line, $\kappa d = 1.5$), $a_2 = 1.4$ (dot-dashed line, $\kappa d = 2$), $a_2 = 1.5$ (dotted line, $\kappa d = 2.5$), by keeping $U_0 = 16$. (b) Flux at the right edge on time with different height, by remaining $a_2 = 1.4$, with $U_0 = 10.5$ (dashed line, $\kappa d = 1.5$), $U_0 = 16$ (dot-dashed line, $\kappa d = 2$), $U_0 = 23$ (dotted line, $\kappa d = 2.5$) to keep κd unchanged, respectively. For all cases $\Psi(x, 0) = \varphi_0(x)$.

that κd remains unchanged. The traversal time of Büttiker and Landauer [20], $t_{BL} = d/\kappa$, given by the barrier width d divided by the "semiclassical" velocity $\kappa = [2(U_0 - E_0)]^{1/2}$, is an important time scale, especially in opaque conditions. With the conservation of κd , t_{BL} is proportional to $1/\kappa^2$. For the specific initial state $\Psi(x, 0) = \varphi_0(x)$, the t_{BL} with the barriers $U_0 = 24$, $U_0 = 16$, and $U_0 = 10$ is 0.05, 0.09, and 0.15, respectively, and with the lowering the barrier, t_{BL} increases. The inset in Fig. 4(a) shows the behavior of the density at the edges. Contrary to $J(a_1, 0) = J(a_2, 0) = 0$, $\rho(a_1, 0)$ and $\rho(a_2, 0)$ are not zero, as the ground state for the potential $U_1(x)$ is not fully localized in the well. It is also shown in Fig. 4(b) that $J(a_1, t)$ dives into the bottom of a negative value and oscillates more strongly. Flux and the density at both edges are not monotonic functions of time. Even if there are some fluctuations, no peak can be clearly distinguished as a precise instant when tunneling begins. The decay time $t_{1/e}$ can be estimated as $1/J_{pl}(a_2)$,

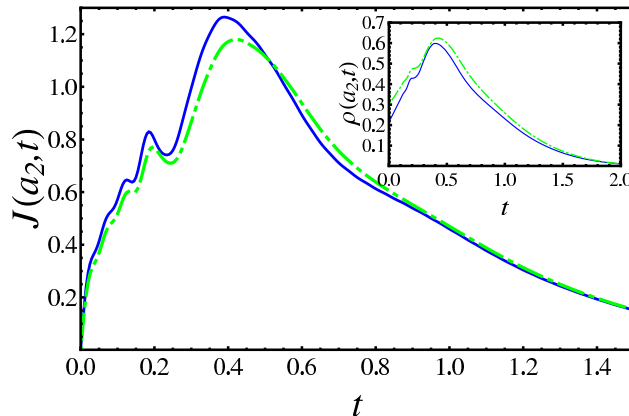


FIG. 6. Time evolution of the flux and the density (in the inset) at the right edge, where the solid line represents the flux (the density in the inset), when $U_0 = 16$ and $a_2 = 1.05$. The dot-dashed line corresponds to the flux (density in the inset) for $U_0 = 10$ and $a_2 = 1.06$. The two barriers are transparent as $\kappa d = 0.25$, and the initial state is $\varphi_0(x)$.

where $J_{\text{pl}}(a_2)$ is the flux at the plateau.

The dependence of the flux at the right edge on time with different width but keeping the height of the barrier $U_0 = 16$ is shown in Fig. 5(a). It is interesting to find that the time that the flux begins to form a plateau is almost equal for different widths, although the flux value at the plateau changes strongly, roughly as $\exp(-2\kappa d)$. In Fig. 5(b), this characteristic time also remains almost unchanged for different U_0 by keeping the same width a_2 .

For comparison, we illustrate the flux and the density at a short time scale for a transparent barrier $\kappa d < 0.25$. It is shown in Fig. 6 that these quantities have similar profiles. They grow from initial to the maximum value and decrease rapidly, contrary to the opaque behavior without an obvious peak. The peak is positioned at $t \approx 0.5$, similar to the time of plateau development in Fig. 5.

In Fig. 7, the time-dependence of the flux (a) and the density (b) at the edges with the initial state $\Psi(x, 0) = \sqrt{2}\sin(\pi x)$ are presented for two different barriers. These two barriers are in the same opaque conditions $\kappa d = 2$. The flux is enhanced by an order of magnitude and oscillates more strongly compared to the initial $\Psi(x, 0) = \varphi_0(x)$, because $\sqrt{2}\sin(\pi x)$ contains larger contributions from different eigenstates. Similarly, the flux at a_2 develops at longer time, when the barrier becomes lower. Different from that with $\Psi(x, 0) = \varphi_0(x)$, the density is zero at $t = 0$ outside the barrier. It can be measured from Fig. 7 (b) that the delay time between the maximum of the density at the right and the left edges is about 0.06 for $U_0 = 16$ and 0.12 for $U_0 = 10$, in a good agreement with above obtained t_{BL} for

these potentials. We conclude that t_{BL} manifests itself as a delay time if over-the-barrier motion becomes essential due to the choice of the initial state. The momentum components that matter at first are the ones larger than $\sqrt{2U_0}$, as the momentum distribution of $\sqrt{2}\sin(\pi x)$ is broad. Moreover, its average local Bohm velocity at the right edge of the barrier $v_B(a_2, t) = J(a_2, t)/\rho(a_2, t)$ decreases from a large value with some oscillations to a relatively stable one close to $\sqrt{2E_0}$ during a short interval, after which the real tunneling starts. This means that the forerunners just go above the barrier instead of tunneling. It is also worth mentioning that the tunneling process for $\Psi(x, 0) = \varphi_0(x)$ occurs indeed from the moment that the decay initiates, because $v_B(a_2, t)$ is always smaller than $\sqrt{2U_0}$.

As discussed in [47, 48] with analytical models, t_{BL} is a characteristic time describing different phenomena, among them over-the barrier transients. This is rather paradoxical, considering its association with “tunnelling” in the defining formula, and has surely not been fully appreciated. A more intuitive understanding of this unexpected role is still missing.

C. Long-term dynamics

After formation of the steady tunneling, the particle probability density shows two distinct features. The first one is an almost uniform change in $\rho(x, t)$ at $x < a_1$ with $\rho(x, t) \approx \rho(x, 0) \exp(-t/t_{1/e})$. The second one can be viewed as a broad bump (wave packet) with relatively small density propagating with the velocity close to $\sqrt{2E_0}$ and spreading in time since it contains all momentum components determined by the $G(k)$ -dependence. In this subsection, we consider the dynamics of the bump at long time scale and trace it to short times.

We assume that the flux $J(X, t)$ and the density $\rho(X, t)$ are measured by a detector located at the distance $X \gg a_2$. It is shown in Fig. 8 for $\Psi(x, 0) = \varphi_0(x)$, that the density at $X \gg a_2$ is nearly zero up to some time, then grows to a sharp maximum, and then decreases at timescales of $t_{1/e}$ with the sequential oscillations due to the diffraction in time phenomenon [27]. The profiles of the flux and density are very similar, with $J(X, t) \approx \sqrt{2E_0}\rho(X, t)$.

In the attosecond experiment analysis [2] the tunneling time was defined as the delay between the time when the barrier begins to be lowered and the time when electron experiences the acceleration by external field. Similarly, we can use the operational phenomenological approach to define a tunneling time as

$$t_{\text{tun},1} = t_X - \frac{X - a_2}{\tilde{v}_p}, \quad (16)$$

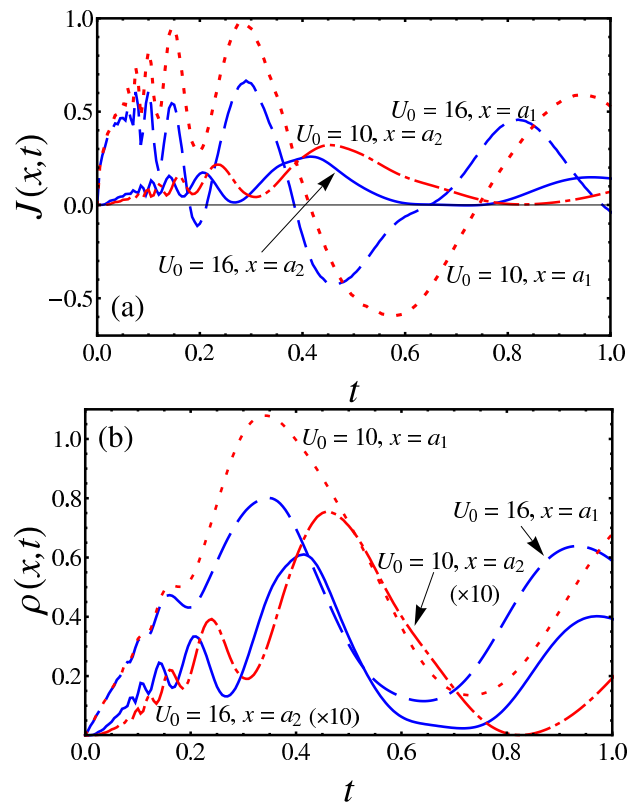


FIG. 7. (a) Flux and (b) density with the barriers $U_0 = 16, a_2 = 1.42$ (solid line at a_2 and dashed line at a_1) and $U_0 = 10, a_2 = 1.63$ (dot-dashed line at a_2 and dotted line at a_1). As the density at a_2 of two barriers is relatively small, it is multiplied by the factor of ten. The two barriers are opaque with $\kappa d = 2$ and the initial state is $\Psi(x, 0) = \sqrt{2} \sin(\pi x)$.

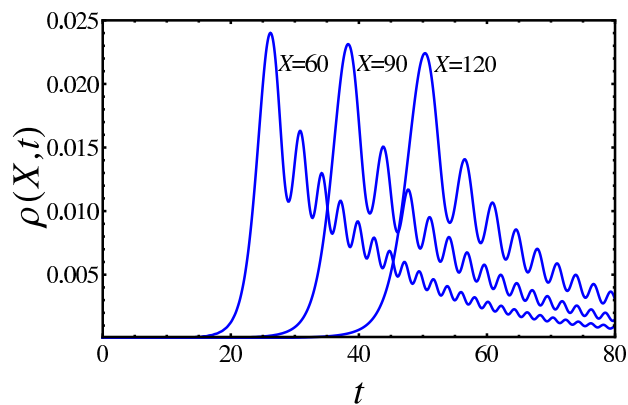


FIG. 8. Time evolution of density $\rho(X, t)$ at given positions $X = 60, 90, 120$, provided that $\Psi(x, 0) = \varphi_0(x)$, $U_0 = 16, a_2 = 1.4$. A strong initial peak is followed by a diffraction in time pattern.

where t_X is the time when the detector measures the strongest first peak of the flux, $\tilde{v}_p = \sqrt{2\tilde{E}_0}$ is the velocity with which the particle moves out of the potential, and the energy

$$\tilde{E}_0 = E_0 - \int_{a_2}^{\infty} U_0 \varphi_0^2(x) dx \quad (17)$$

is a slightly less than E_0 , as the potential changes suddenly from $U_1(x)$ to $U_2(x)$. As t_X , a measurable quantity, represents the time that the particle is detected, the tunneling time can be calculated by Eq. (16). For instance, for $\Psi(x, t = 0) = \varphi_0(x)$, $U_0 = 16$, $a_2 = 1.4$, when the detector is at $X = 120$, then $t_X = 50.3$, and resulting $t_{\text{tun},1} = 5.62$. A variant, similar to Eq.(16), is to calculate the tunneling time as

$$t_{\text{tun},2} = t_X - \frac{X - a_2}{v_X}, \quad (18)$$

where v_X is the velocity of the flux peak. For example, $v_X = 2.517$ as defined by the motion from $X = 120$ to $X = 122$. According to Eq.(18), the corresponding tunneling time is $t_{\text{tun},2} = 3.18$. As it can be assumed that the velocity of the electron is constant outside the barrier in a classical manner, we can conclude that the tunneling time extracted from the measurements by a remote detector is X -independent. Both Eq.(16) and Eq.(18) extrapolate electron motion from distance to the exit of the tunneling process. However, these two times are not equal either to the time of formation of the steady tunneling in Fig. (4) or to the decay time $t_{1/e}$.

Fig. 9 depicts how the flux evolves with time and distance at two timescales for $\Psi(x, 0) = \varphi_0(x)$. The curvature of the maximum flux region in Fig. 9(a) shows that it takes some time for the flux to develop a constant speed in free space. If we trace the electron from far distances based on the data shown in Fig. 9(b) back to the right edge of the barrier, we obtain the tunneling time 3.1 for $\Psi(x, t = 0) = \varphi_0(x)$, $U_0 = 16$, $a_2 = 1.4$, very close to $t_{\text{tun},2} = 3.18$. However, the tunneling time measured at a_2 is not zero but a small positive value as the peak of the flux appears at $t \approx 1$, seen in Fig. 9(a). It is also different from $t_{\text{tun},1} = 5.62$ and $t_{\text{tun},2} = 3.18$ extrapolated from $X = 120$.

It is expected in some models that the wave function at long times and distances can be obtained with the stationary phase approximation. Eq. (3) in this limit can be recast as

$$\Psi(x > a_2, t) \approx \frac{1}{\sqrt{2\pi i}} \int_0^{\infty} G(k) \exp \left\{ i \left[\theta(k) + kx - \frac{k^2 t}{2} \right] \right\} dk, \quad (19)$$

and the phase $\theta(k) + kx - k^2 t/2$ can be expanded near the stationary point K satisfying the equation $(d\theta(k)/dk)_{k=K} + x - Kt = 0$. However, $G(k)$ in our calculations is not a sufficiently smooth function near the K -points due to the

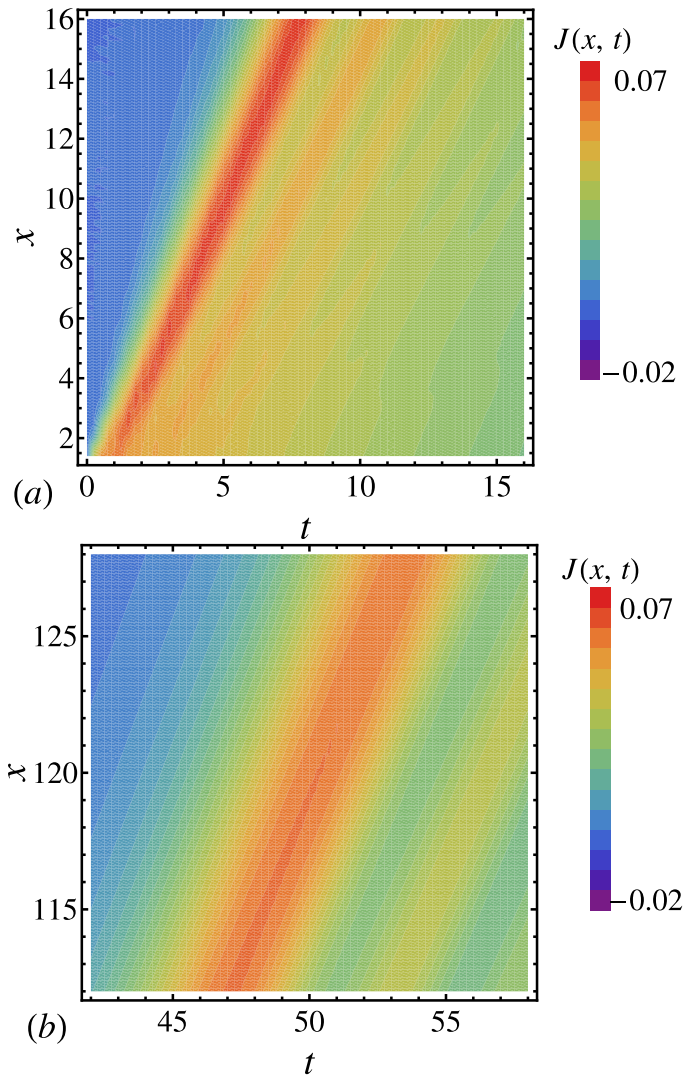


FIG. 9. The flux outside the barrier versus time and position after a short time near the right edge of the barrier (a) as well as after a long time far away from the right edge of the barrier (b). All the parameters are the same as in Fig. 8.

resonances shown in Fig. 2. Therefore, the stationary phase approximation does not provide a satisfactory description of the peak propagation.

Another factor that affects the tunneling time is the closing time t_0 , when the potential turns back from $U_2(x)$ to $U_1(x)$ and the tunneling is interrupted. The time evolution of the flux observed at the same remote position of detector with different closing times $t_0 = \infty$, $t_0 = (1/3)t_{1/e}$, $t_0 = (1/6)t_{1/e}$, $t_0 = (1/9)t_{1/e}$ is demonstrated in Fig. 10(a), and $t_{1/e}$ is the life time introduced above. The peak of the flux with shorter closing time t_0 appears earlier than that with longer t_0 , as a result of the increased energy spreading [49]. It is shown in Fig. 10(b) that after closing

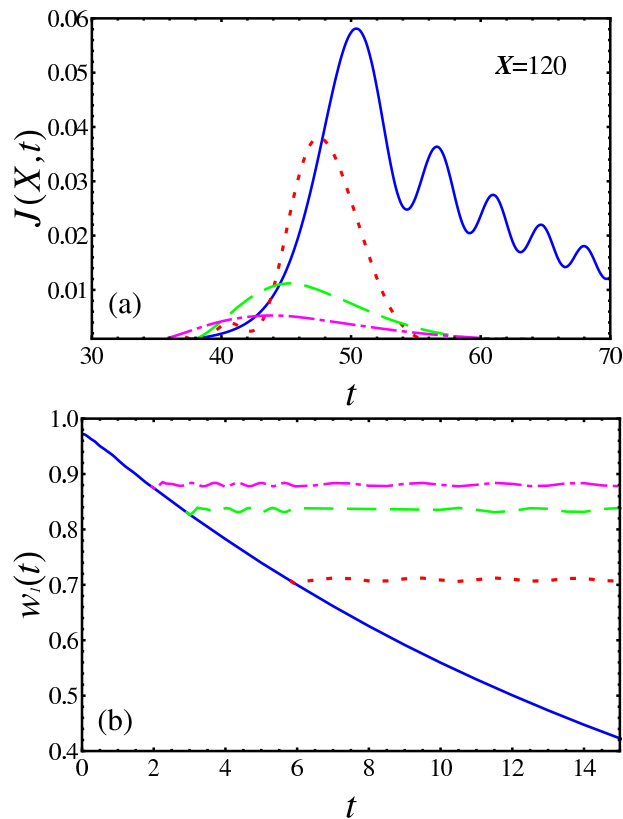


FIG. 10. (a) Flux as a function of time detected at $X = 120$ and (b) $w_1(t)$ with different closing time $t_0 = \infty$ (solid), $t_0 = (1/3)t_{1/e}$ (dotted), $t_0 = (1/6)t_{1/e}$ (dashed), $t_0 = (1/9)t_{1/e}$ (dot-dashed), $t_{1/e}$ is the life time for the particle in the case of $t_0 = \infty$. Other parameters are the same as those in Fig. 8.

the barrier, the probability to find the particle in the well remains almost unchanged. This shows that components with larger momenta tunnel through the barrier first.

IV. CONCLUSIONS

We have studied numerically exactly the tunneling and further propagation of an initially localized particle through a barrier of finite height and width. The barrier considered is opaque, however, not extremely so, to ensure a reasonable tunneling probability and the decay time $t_{1/e}$ of the order of $100E_0^{-1}$, where E_0 is the energy of the initial state. The probability density evolution on a short time scale, that is much less than the decay time, depends strongly on the initial state. Dependent on how this state is prepared, this short-term motion can include both under-the-barrier tunneling and over-the-barrier propagation, as seen in the evolution of the density and flux at the barrier edges.

The tunneling starts instantly, however, some time is required to develop the outgoing flux. As expected, there is a time delay between the flux development at the left and the right edges of the barrier. If the initial state is close to the ground state of the potential at $t < 0$, the timescale of the flux development is much longer than the Büttiker-Landauer traversal time expected for the given barrier parameters and is determined by the components of the initial wavefunction. However, if the initial state is more tightly localized, the Büttiker-Landauer time manifests itself as a time delay of the flux and density maxima between the left and right edges of the barrier.

In the long-term behavior we have considered the propagation of the escaped wave packet at the distances much larger than the scale of the potential. The shape of the density distribution within the potential remains intact even at longer times. From the operational definition of the escape time, related to the position of the maximum of the wave packet density, we have estimated the time the particles escaped from the potential. This time is also much longer than the traversal time for the given barrier. To determine the effect of the time dependence of the barrier, we also implemented escape time windows considerably shorter than $t_{1/e}$. The extrapolated time estimated for the closing potentials is smaller than that for the potentials permanently open, showing that the increasing importance of faster components for shorter time windows. An interesting side effect of the analysis is that decay by a moderately opaque barrier (permanently open) may be an excellent way to observe the elusive diffraction in time phenomenon [26]. A detailed analysis of the diffraction in time accompanying the tunneling will be presented elsewhere.

V. ACKNOWLEDGEMENT

E.Y.S. and J.G.M. are grateful to the support of University of Basque Country UPV-EHU (Grant GIU07/40), Basque Country Government (IT-472-10), and Ministry of Science and Innovation of Spain (FIS2009-12773-C02-01). M. B. is supported by the Swiss NSF, MaNEP, and the European ITN, NanoCTM.

-
- [1] G. Gamow, *Z. Phys.* **51**, 204 (1928); R. W. Gurney and E. U. Condon, *Phys. Rev.* **33**, 127 (1929).
 [2] P. Eckle, A.N. Pfeiffer, C. Cirelli, A. Staudte, R. Döner, H.G. Müller, M. Büttiker, and U. Keller, *Science* **322**, 1525 (2008).

- [3] E. H. Visscher, J. Lindeman, S. M. Verbrugh, P. Hadley, J. E. Mooij, and W. van der Vlueten, *Appl. Phys. Lett.* **68**, 2014 (1996).
- [4] E.R. Brown, J.R. Söderström, C. Parker, L.J. Mahoney, K.M. Molvar, and T.C. McGill, *Appl. Phys. Lett.* **58**, 2291 (1991)
- [5] S. Slivken, Z. Huang, A. Evans, and M. Razeghi, *Appl. Phys. Lett.* **80**, 4091 (2002).
- [6] D. M. Stamper-Kurn, H.-J. Miesner, A. P. Chikkatur, S. Inouye, J. Stenger, and W. Ketterle, *Phys. Rev. Lett.* **83**, 661 (1999).
- [7] L. A. MacColl, *Phys. Rev.* **40**, 621 (1932).
- [8] E. P. Wigner, *Phys. Rev.* **98**, 145 (1955).
- [9] T. E. Hartman, *J. Appl. Phys.* **33**, 3427 (1962).
- [10] H. G. Winful, *Phys. Reports* **436**, 1 (2006).
- [11] V. Gasparian, T. Christen, and M. Büttiker, *Phys. Rev. A* **54**, 4022 (1996); M. Büttiker, *J. Phys. (Pramana)* **58**, 241 (2002).
- [12] R. Landauer and Th. Martin, *Rev. Mod. Phys.* **66**, 217 (1994).
- [13] *Time in Quantum Mechanics*, Ed. by J. G. Muga, R. Sala Mayato, and I. L. Egusquiza (Springer, Berlin, 2002)
- [14] N. Tombros, C. Jozsa, M. Popinciuc, H. T. Jonkman, and B. J. van Wees, *Nature (London)* **448**, 571 (2007).
- [15] R. A. Sepkhanov, M. V. Medvedyeva, and C. W. J. Beenakker, *Phys. Rev. B* **80**, 245433 (2009).
- [16] F. T. Smith, *Phys. Rev.* **118**, 349 (1960).
- [17] M. Büttiker, *Phys. Rev. B* **27**, 6178 (1983).
- [18] A. I. Baz, *Yad. Fiz.* **5**, 229 (1967).
- [19] V. F. Rybachenko, *Yad. Fiz.* **5**, 895 (1967).
- [20] M. Büttiker and R. Landauer, *Phys. Rev. Lett.* **49**, 1739 (1982).
- [21] D. V. Khomitsky and E. Ya. Sherman, *Europhys. Lett.* **90**, 27010 (2010).
- [22] B. Huang and I. Appelbaum, preprint arXiv:1007.0233.
- [23] A. M. Steinberg and R. Y. Chiao, *Phys. Rev. A* **49**, 3283 (1994).
- [24] S. Brouard, R. Sala, and J. G. Muga, *Phys. Rev. A* **49**, 4312 (1994).
- [25] M. Büttiker and H. Thomas, *Ann. Phys. (Leipzig)* **7**, 602 (1998).

- [26] A. del Campo, G. García Calderón, and J. G. Muga, *Phys. Rep.* **476**, 1 (2009).
- [27] M. Moshinsky, *Phys. Rev.* **88**, 625 (1952).
- [28] J. M. Martinis, M. H. Devoret, D. Esteve, and C. Urbina, *Physica B* **L52** 159 (1988).
- [29] P. Gueret, E. Marclay, and H. Meier, *Appl. Phys. Lett.* **53** 1617 (1988).
- [30] S. K. Sekatskii and V. S. Letokhov, *Phys. Rev. B* **64**, 233311 (2001).
- [31] A. M. Steinberg, P. G. Kwiat, and R. Y. Chiao, *Phys. Rev. Lett.* **71**, 708 (1993).
- [32] Ch. Spielmann, R. Szipöcs, A. Stingl, and F. Krausz, *Phys. Rev. Lett.* **73**, 2308 (1994).
- [33] A. M. Steinberg, *Lect. Notes Phys.* **734**, 333 (2008).
- [34] D. Mugnai and A. Ranfagni, *Lect. Notes Phys.* **734**, 355 (2008).
- [35] A. del Campo, F. Delgado, G. García-Calderón, J. G. Muga, and M. G. Raizen, *Phys. Rev. A* **74**, 013605 (2006).
- [36] A. Marchewka and E. Granot, *Phys. Rev. A* **79**, 012106 (2009).
- [37] G. Kälbermann, *Phys. Rev. C* **79**, 024613 (2009), G. Kälbermann, *Phys. Rev. C* **77**, 041601 (2008).
- [38] N. G. Kelkar, H. M. Castañeda, and M. Nowakowski, *EPL* **85**, 20006 (2009).
- [39] D. Sokolovski, *Lect. Notes Phys.* **734**, 195 (2008).
- [40] M. Büttiker, H. Thomas, and A. Pretre, *Phys. Lett. A* **180**, 364 (1993).
- [41] J. Gabelli, G. Feve, J.-M. Berroir, B. Placais, A. Cavanna, B. Etienne, Y. Jin, and D. C. Glattli, *Science* **313**, 499 (2006).
- [42] S.E. Nigg, R. Lopez, and Markus Büttiker, *Phys. Rev. Lett.* **97**, 206804 (2006).
- [43] G. Féve, A. Mahé, J.-M. Berroir, T. Kontos, B. Placais, D.C. Glattli, A. Cavanna, B. Etienne, and Y. Jin, *Science* **316**, 1169 (2007).
- [44] M. Moskalets, P. Samuelsson, and M. Büttiker, *Phys. Rev. Lett.* **100**, 086601 (2008).
- [45] J. Keeling, A. V. Shytov, and L. S. Levitov, *Phys. Rev. Lett.* **101**, 196404 (2008).
- [46] M. Büttiker and M. Moskalets, *Int. Journ. Mod. Phys. B* **24**, 1555 (2010).
- [47] J. G. Muga and M. Büttiker, *Phys. Rev. A*, **62**, 023808 (2000).
- [48] F. Delgado, J. G. Muga, A. Ruschhaupt, G. García-Calderón, and J. Villavicencio, *Phys. Rev. A* **68**, 032101 (2003).
- [49] A. del Campo, J. G. Muga and M. Moshinsky, *J. Phys. B: At. Mol. Opt. Phys.* **40**, 975 (2007).